Binary Mixture of Nonadditive Hard Spheres Adsorbed in a Slit Pore: A Study of the Population Inversion by the Integral Equations Theory

A. Ayadim and S. Amokrane*

Physique des Liquides et Milieux Complexes, Faculté des Sciences et Technologie, Université Paris-Est (Créteil), 61 Av. du Général de Gaulle, 94010 Créteil Cedex, France

Received: July 30, 2010; Revised Manuscript Received: October 27, 2010

The structure of a binary mixture of nonadditive hard spheres confined in a slit pore is studied by the integral equations method in which the confining medium acts as a giant particle at infinite dilution. The adsorption/desorption curves are studied as a function of the composition and density, when the homogeneous bulk mixture is near the demixing instability. The Ornstein−Zernike integral equations are solved with the reference functional approximation closure in which the bridge functions are derived from Rosenfeld's hard sphere functional for additive hard sphere. To study the high composition asymmetry regime in which a population inversion occurs, we developed an approximate closure that overcomes the no solution problem of the integral equation. By comparison with simulation data, this method is shown to be sufficiently accurate for predicting the threshold density for the population inversion. The predictions of simpler closure relations are briefly examined.

1. Introduction

In domains ranging from separation processes to nanotechnology, a prior knowledge of the role of the physicochemical parameters on the behavior of adsorbed fluids as well as the influence of the latter on the properties of the adsorbing medium is of great value in view of specific applications. This motivated a vast literature devoted to the theoretical study of confined fluids (see, for instance, ref 1 and references therein). For the theory itself, confined fluids provide additional (and often more stringent) tests, in comparison with homogeneous ones. Since their study is accordingly more complex, it is reasonable to start with simple models. An example is the mixture of nonadditive hard spheres (NAHS) confined between two parallel smooth walls modeling a slit pore. Besides its convenience for the theory, this popular model captures the main features of pseudobinary mixtures of hard-sphere-like colloidal particles, modeling, for instance, sterically stabilized dispersions or charged stabilized ones in the regime of high salt concentration. Despite its simplicity, this model shows a quite rich behavior, depending on the size or composition asymmetry. Even in the case of equal diameters, a slight nonadditivity favors the demixing phase separation in the bulk. The homogeneous NAHS mixture has thus been the subject of numerous studies both by the integral equations (IE) method[2] based on the Ornstein−Zernike equations (OZE) and by simulation and other thermodynamic methods; see, for example, refs 3−7 and references therein for size symmetric mixtures and refs 8−14 for asymmetric ones.

More recently, the behavior of the NAHS mixture in confined geometry has been considered in refs 15−18; see also ref 19 for the extreme case of the Widom−Rowlinson mixture. When combined with the effect of confinement, the bulk instability leads to a more complex behavior, including a selective adsorption in the pore of the minority species. When the pore is in equilibrium with a NAHS mixture highly asymmetric in composition and close to bulk demixing, a population inversion occurs in the pore when the total bulk density ρ_b is varied: a jump in the adsorption of the minority species occurs after reaching a threshold value close to the coexistence density ρ_b^{coex}, and vice versa for the majority species.[17,18] The population of the pore by the different species becomes the inverse of that of the bulk. More recently, it was shown in our group that a similar effect could be triggered by an external field, when one of the species bears a dipole moment.[20,21] This leads, in the pore, to a field induced population inversion near the bulk instability (referred to in ref 21 as the F-PINBI effect). One may accordingly produce a jump in the physical properties of the fluid filled pore, by the sole action of the external field, an effect with potentially numerous applications.

This F-PINBI effect has been evidenced by Monte Carlo (MC) simulation. It is however difficult to investigate in this way a wide domain of the parameters space. It is also clear that, even for the simple confined mixture of hard spheres and dipolar hard spheres considered in refs 20 and 21, one has to deal with an inhomogeneous asymmetric mixture, anisotropic interactions that complicate the semianalytic approach. This is why it seems useful to continue the effort to develop sufficiently accurate methods on simpler situations, in the spirit of the previous studies of NAHS mixtures (see, for example, Kim et al.[18] who used the IE of Jagannathan et al.,[5] Jimenez et al.[17] for the Percus−Yevick/hypernetted chain (PY/HNC) closure of the OZE, or ref 16 for the replica method). In all these studies, the closure of the OZE is of central importance. In this respect, other studies have shown that the reference HNC integral equation based on the knowledge of the free energy functional for some reference system is very useful. This is the case with the approach pioneered by Rosenfeld,[22] who proposed to use for the unknown *bridge* functional that of additive hard spheres (HS), the so-called fundamental measures functional (FMF). For shortness, we will refer to this variant of the RHNC IE as the reference functional approximation (RFA). In the same theoretical framework, Schmidt[10] has generalized the FMF to nonadditive hard spheres. He has shown that the NAHS functional gives an accurate description of the structure when the direct correlation functions (dcfs) computed as the second functional derivatives are inserted in the OZE. However, we have recently shown[12] that this approach is not completely satisfactory when

10.1021/jp107157a
Published on Web 11/23/2010

used to compute the structure in the test-particle limit. This is why we will use here the FMF in its original form. In the bulk, the situation is the following one: with the integral equations other than the RFA, the critical behavior of the NAHS mixture cannot yet be studied quantitatively for a range of nonadditivities (see, for example, refs 3 and 7; the alternative method used in ref 9 might be more efficient, but the case of size symmetric mixtures was not discussed there). In its turn, the RFA which is usually accurate for quite disparate potentials suffers from the no-solution problem that precludes the determination of the complete phase diagram. In this work, we will hence focus on the structure of the confined fluid and the population inversion effect, which require reasonably accurate bulk direct correlation functions on a narrower domain of the parameters space. We will then show that this can be achieved through a variant of the RHNC/RFA that has a much wider domain of convergence while being intermediate between the latter and the PY/HNC closure. We can study in this way the population inversion effect, without having to determine the entire bulk phase diagram. To this end, this paper is organized as follows: in section II, we present the RFA method and the Δb approximation we have developed to overcome the no-solution problem. In section III, we first test the method on the bulk structure in two representative state points. We next examine the structure of the confined mixture, including a comparison of the density profiles and adsorption curves with simulation data. We end this paper with a short conclusion.

2. Theoretical Background

2.1. The Model. We consider a binary mixture of nonadditive hard spheres confined between two parallel perfectly smooth walls, separated by a distance H. All particles interact with the walls with the hard sphere potential $\phi_{wi}^{HS}(z)$ (the center of the particle lies in the range $[^1/_2\sigma, H - {}^1/_2\sigma]$). In the NAHS mixture, all particles interact with the hard sphere potential ϕ_{ij}^{HS} ($r \leq \sigma_{ij}$) $= \infty$, ϕ_{ij}^{HS} ($r > \sigma_{ij}$) $= 0$, but the hard sphere diameter between unlike particles is $\sigma_{12} = {}^1/_2(\sigma_{11} + \sigma_{22})(1 + \delta)$. We will consider here a positive nonadditivity, since it favors the demixing in the bulk, a condition for observing the phenomenon of population inversion. The fluid in the pore is assumed to be in equilibrium with a bulk mixture. We denote by ρ_i and x_i the density and the concentration of species i in the bulk. In what follows, species 2 will be the minority one in the bulk. We will be especially interested in the high composition asymmetry $x_2 \sim 0.02$ (for simplicity, we considered only size symmetric mixtures with $\sigma_{11} = \sigma_{22} \equiv \sigma$).

This model should be appropriate to a real slitlike pore whose lateral dimensions are much larger than the separation H between the walls and that exchanges particles with a reservoir through an interfacial region much smaller than the remainder of the pore. The physical mixtures closest to this model are pseudobinary mixtures of sterically stabilized colloids (or charged ones with very short Debye length), without preferential interaction with the pore walls (for the smooth wall approximation to be valid, the wall should be made of much smaller particles than the colloidal ones).

2.2. Structure of the Confined Mixture from Integral Equations. The integral equations for the pair structure start from the OZE:[2]

$$\gamma_{ij} = \sum_k \rho_k c_{ik} \otimes h_{kj} \tag{1}$$

where $\gamma_{ij} = h_{ij} - c_{ij}$ and $\otimes$ designates a convolution product: $[f \otimes g](\mathbf{r}) = \int d\mathbf{r}' f(\mathbf{r}')g(\mathbf{r}' - \mathbf{r})$. $h_{ij} = g_{ij} - 1$ is the total correlation function, and c_{ij} is the direct correlation function (dcf). The OZE must be supplemented by closure relations.

$$g_{ij} = \exp\{-\beta\phi_{ij} + h_{ij} - c_{ij} - b_{ij}\} \tag{2}$$

This formally exact relation must be supplemented in practice by an approximation for the bridge function b_{ij}. To study an inhomogeneous fluid by this method, one considers the confining medium as an additional particle at infinite dilution, that creates a potential ϕ_{iw} on the particles of the fluid. For a slit pore, the potential $\phi_{iw}(z)$ is the limit for $R \to \infty$ of the potential generated by a spherical shell of radii R and $R + H$. The basic quantities we are interested in are the density profiles $\rho_i(z) = \rho_i g_{iw}(z)$ from which we compute the normalized adsorption of species i defined as

$$\Gamma_i = \frac{1}{H}\int_0^H \rho_i(z)\, dz \tag{3}$$

The wall-particle two-body correlation functions $g_{iw}(z)$ for $i = 1, 2$ are given by the closures of the wall-particles OZEs

$$g_{iw}(z) = \exp(-\beta\phi_{iw} + \gamma_{iw} - b_{iw}) \tag{4}$$

with

$$\gamma_{1w} = \rho_1 c_{11} \otimes h_{1w} + \rho_2 c_{12} \otimes h_{2w} \tag{5}$$

$$\gamma_{2w} = \rho_1 c_{21} \otimes h_{1w} + \rho_2 c_{22} \otimes h_{2w} \tag{6}$$

The direct correlation functions c_{ij} in the bulk are obtained from the equations for the homogeneous mixture:

$$\begin{aligned} \gamma_{11} &= \rho_1 c_{11} \otimes h_{11} + \rho_2 c_{12} \otimes h_{21} \\ \gamma_{12} &= \rho_1 c_{11} \otimes h_{12} + \rho_2 c_{12} \otimes h_{22} \\ \gamma_{22} &= \rho_1 c_{21} \otimes h_{12} + \rho_2 c_{22} \otimes h_{22} \end{aligned} \tag{7}$$

with three closures for g_{ij} in eq 2. These are rather standard equations which can be solved with different algorithms, with the simplest one being the direct iterations. It suffices here to notice that the actual input is the bridge function b_{ij} discussed below.

2.3. The RFA Closure and the Δb Approximation. Several studies from different groups have shown that the approach that starts with Rosenfeld's[22] functional for additive hard spheres, plus possibly a mean field treatment of non-HS contributions, is quite successful for studying the structure of homogeneous and inhomogeneous fluids. In most of its uses, the structural quantities are directly determined from the minimization of the grand potential functional (see, for example, the reviews on the density functional theory (DFT) in refs 23 and 24). Another aspect which has been less recognized, however, is that, in the integral route, the same approach can be used to obtain the bridge function from the HS *bridge* functional whose definition is recalled in Appendix A (see also references in ref 25 for other alternatives). This IE with RFA closure actually provides a generic and accurate method for studying a wide variety of interaction potentials, well beyond the mean-field treatment of the standard DFT. Indeed, as opposed to the latter treatment of the attractions, the entire potential is incorporated directly

in the closure relations (the only approximation being at the level of the bridge function). Besides the HS mixture,[26] it has been used to study the Lennard-Jones (LJ) fluid,[27] slightly asymmetric mixtures with various interactions,[8] the potential of mean force (PMF) for colloids in the bulk[28] and in confined geometry,[29,30] the drying phenomenon,[31] and spherically averaged anisotropic potentials.[32] We have recently shown[33] how it can be used (under the RFA designation) to compute bulk free energies. The result improves upon the standard approximation of the nonlocal term in the RHNC theory of Lado[34,35] and provides a more consistent criterion for determining the reference system HS diameters.

Although being capable of treating a variety of interaction potentials, the resulting integral equations unfortunately suffer from the problem of the no-solution domain, common to most integral equations of the HNC type (see, for example, refs 36−38). In refs 39 and 40, we proposed possible means to circumvent it which are, however, not efficient in the present conditions (we also cannot use the generalized FMF, as discussed in ref 12). The nonconvergence concerns here the computation of the bulk structure. It occurs when the total density ρ increases, in the high composition asymmetry $x_2 \ll 1$ relevant to the phenomenon of population inversion. The radial distribution function of the minority species $g_{22}(r)$ shows then a large peak at contact which grows until divergence of the algorithm, irrespective of the numerical details (initial values, mesh size, number of integration points, etc.). This peak in $g_{22}(r)$ (which in particular cannot be reproduced in the first iteration) goes with a similar one in the direct correlation function $c_{22}(r)$. To devise an approximate closure that is more stable, this too rapid growth of $g_{22}(r)$ must be reduced. We were thus guided by the fact that the Percus−Yevick approximation, for which all the $c_{ij}(r)$ are zero beyond the hard cores, still gives at least qualitatively correct results for $g_{22}(r)$ and presents a much wider convergence domain for the case of the NAHS mixture considered here. We thus need a closure in between PY and the RFA one, this only *beyond* the hard cores. To simplify the notations, we drop for the moment the species indexes and the r dependence. By introducing the indirect correlation function $\gamma = h - c$, we note that the dcf $c = h - \gamma = g - (\gamma + 1)$ can be written formally in terms of the PY quantities as

$$c = g^{\mathrm{PY}} \exp(b^{\mathrm{PY}} - \gamma^{\mathrm{PY}}) \exp(\gamma - b) - (\gamma + 1) \quad (8)$$

or by introducing the difference between the PY and the RFA bridge functions $\Delta b \equiv b^{\mathrm{PY}} - b$ as

$$c = g^{\mathrm{PY}} \exp(\Delta b) \exp(\gamma - \gamma^{\mathrm{PY}}) - (\gamma + 1) \quad (9)$$

Recalling now that the indirect correlation function is continuous even at the hard core, it seems reasonable to consider that the difference between c and c^{PY} beyond the hard core (recall that the latter is there equal to zero) comes first from the difference Δb in the bridge functions. One may thus take, *at this stage*, $\gamma \simeq \gamma^{\mathrm{PY}}$ beyond the hard core. Hence, by noting that then $g^{\mathrm{PY}} = \gamma^{\mathrm{PY}} + 1$, outside the hard core, one finally gets

$$\begin{array}{ll} c = (1 + \gamma^{\mathrm{PY}})(\exp(\Delta b) - 1) & r > \sigma \\ g = 0 & r \leqslant \sigma \end{array} \quad (10)$$

Since it emphasizes the change in the bridge function from its PY value, we shall refer to this approximation as the Δb closure. In the composition asymmetric mixture, the Δb closure is used for computing g_{22} while the full RFA closure is retained for g_{11} and g_{12}. To compute Δb_{22}, one has to evaluate $b_{22}[h_{ij}]$ from the FMF functional, as outlined in the Appendix B, and $b_{22}^{\mathrm{PY}} = \gamma_{22}^{\mathrm{PY}} - \ln(1 + \gamma_{22}^{\mathrm{PY}})$. The algorithm must thus solve first the PY closure for the mixture to obtain the input for the Δb closure.

Finally, one has to determine the reference system hard sphere diameters $\tilde{\sigma}_{ij}$ (these are actually not adjustable parameters[41] in the usual sense). For the full RFA closure, the optimum diameter is obtained from the Lado criterion,[34] or from its generalization derived in ref 33 that is more consistent with the RFA. Since the Δb approximation is not strictly consistent with the RFA (or RHNC) free energy, we cannot use Lado's criterion or its generalization.[33] We thus used the virial-compressibility consistency:

$$\left(\frac{\partial \beta P}{\partial \rho_i}\right)_T = 1 - \rho \sum_j x_j \tilde{c}_{ij}(k = 0) \quad (11)$$

where P is the virial pressure and $\tilde{c}_{ij}(k)$ is the Fourier transforms of the dcfs. Note that the dependence on density of the optimum diameter makes a negligible contribution to $(\partial \beta P/\partial \rho_i)_T$. It is thus ignored in practice (see, for example, ref 3 for a similar procedure with other integral equations). These two partial compressibility criteria ($i = 1, 2$) allow the determination of the two reference hard sphere diameters. Finally, for the wall particle closure, we used the RFA closure with the optimum diameters obtained in the bulk, since we did not encounter the no-solution domain in the conditions considered here. The necessity to solve the integral equations for each set of reference diameters together with the computation of the FMF bridge functions in the bulk then in the pore makes this method rather lengthy. The results we have obtained in this way in some representative cases are discussed in the next section.

3. Results

3.1. Bulk Pair Structure. Studying the behavior of a homogeneous NAHS mixture was not the objective in this work. but the bulk dcfs are required to compute the structure of the confined fluid. We thus first tested the quality of the integral equation in the bulk. In Figure 1, the radial distribution functions for a symmetric NAHS mixture with $x_2 = x_1 = 0.5$ are compared with the simulation data of ref 5. For such a symmetric mixture, Figure 1 confirms the excellent behavior of the RFA closure, already observed in refs 8 and 12. The behavior of the Δb closure is also quite satisfactory, in between PY and RFA, as expected. These conditions are however not demanding enough for our purpose, as evidenced at higher composition asymmetry, an illustration of which is shown in Figure 2. For $x_2 = 0.02$, the mixture is very dilute in species 2. At the density $\rho^* = \rho\sigma^3 = 0.45$, g_{22} starts to show the large values near contact discussed above. At the RFA no-solution boundary, the value of g_{22} is about 14, whereas the value obtained with the Δb approximation is slightly lower. The convergence domain of the latter is accordingly larger. It should be stressed that this high composition asymmetry is quite demanding since the integral equation must be accurate enough to treat a mixture in which the density of the minority component is $\rho_2^* = 0.009$. The quality of the Δb closure is lower but still significantly better than the PY one. Note in Figure 2b the tails beyond the hard cores, absent in the PY closure. The latter shows more negative values inside the cores, which compensates somehow the absence of the

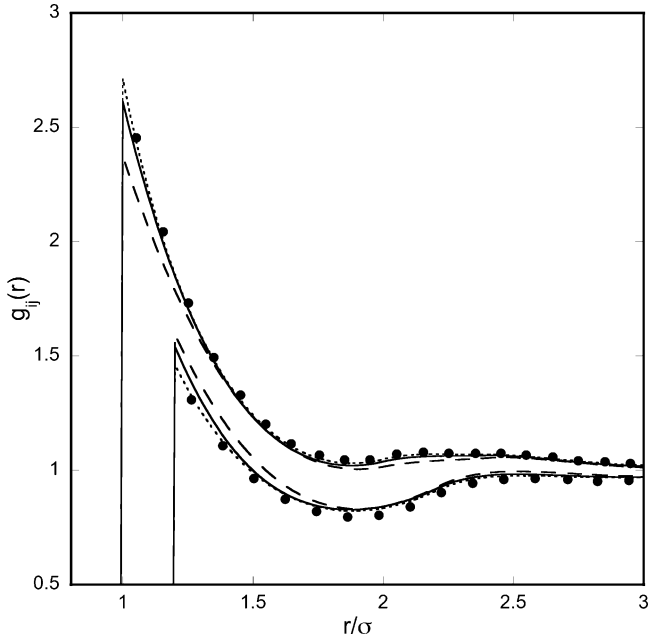

Figure 1. Radial distribution functions for symmetric NAHS mixture with $\delta = 0.2$, $\rho^* = 0.376$, and $x_2 = 0.5$. Dotted lines, RFA; solid lines, Δb; dashed lines, PY; symbols, MC results.[5]

positive tail in the dcf (the dominant contributions to the convolutions in eq 7 come from regions where c and h have the same sign).

3.2. Structure of the Confined Mixture.

3.2.1. Evaluation of the Integral Equation for the Structure of an Inhomogeneous Fluid. The quality of the IE with RFA closure has been discussed in refs 29−31 on various models. Before studying the NAHS mixture, we considered the hard core Yukawa fluid recently studied in refs 41, 43, and 44 to further evaluate it. The interaction potential is then

$$\phi(r) = \infty, \quad r \le \sigma; \quad \phi(r) = -\varepsilon \frac{e^{-\kappa(r/\sigma - 1)}}{r/\sigma}, \quad r > \sigma \tag{12}$$

Figure 3 shows density profiles for a Yukawa fluid near a single wall, and Figure 4 in a pore of width $H = 4\sigma$. The upper curve in Figure 3 is for an adsorbing wall (see Figure 6 in ref 43 for the value of the different parameters). The RFA/RFA closure is in very good agreement with simulation. It is even better than the modified mean-field DFT[43] (to better treat the attractions). The lower curve is for the same fluid but near a hard wall. The behavior of the RFA/RFA closure confirms again the improvement upon a mean-field treatment. The medium curve corresponds to one of the situations considered in refs 41 and 44. The RFA/RFA closure is in very good agreement with simulation when the optimum diameter for the pore-fluid bridge function is obtained from the contact value theorem $P = k_B T \rho(\sigma)$, where P is the bulk pressure. For $\rho^* = 0.79984$, we find $P/\rho k_B T = 1.32$. The contact value theorem density is verified for an optimum diameter $\tilde{\sigma} = 0.9673\sigma$ (its value in the bulk is $\tilde{\sigma} = 0.9720\sigma$). It should be noted that it is particularly difficult to obtain an accurate contact value (see eq 4) in this case, since the contribution of the bridge function $b(z)$ cancels nearly exactly that of the indirect correlation function $\gamma(z)$. In ref 41, the contact value $\rho(\sigma)$ shown for the same state point differs notably from the simulation one, either because this constraint is not obeyed or because of an inaccurate bulk pressure.

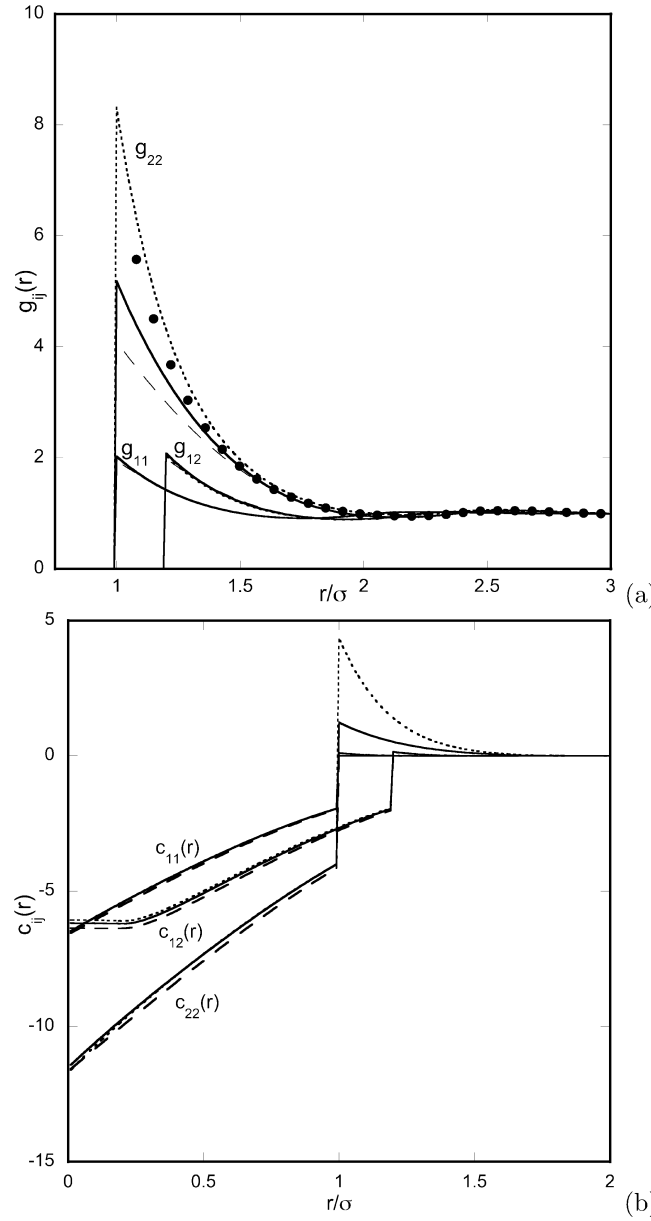

Figure 2. (a) Radial distribution functions for a composition asymmetric NAHS mixture. The parameters are $\delta = 0.2$, $\rho^* = 0.45$, and $x_2 = 0.02$. Dotted lines, RFA; solid lines, Δb; dashed lines, PY; symbols, MC.[42] (b) Direct correlation functions corresponding to (a).

In Figure 4 now, we show the result for one of the state points for which a large deviation was found in ref 41 between simulations and theory. We have repeated the simulation for this state point (details will be given elsewhere; see also ref 21 for the technical details). In contrast with the method used in ref 44, the grand canonical simulation in the pore is performed with the chemical potential determined from a (N,V,T) simulation of a bulk fluid having the density $\rho^* = 0.70063$ given in ref 44 and used in ref 41. The results obtained in this way (circles) depart significantly from those of ref 44 (squares). Contrarily to the case of ref 41, we then find a good agreement between simulation and the IE with RFA closure (incidentally, the theoretical results with the method of ref 41 are now closer to simulation). The difference between the two simulations might be due to an inaccurate correspondence between the bulk density and the chemical potential obtained from an analytical equation of state.

3.2.2. Density Profiles. While these additional tests confirm the overall quality of the full RFA closure, it suffers as recalled

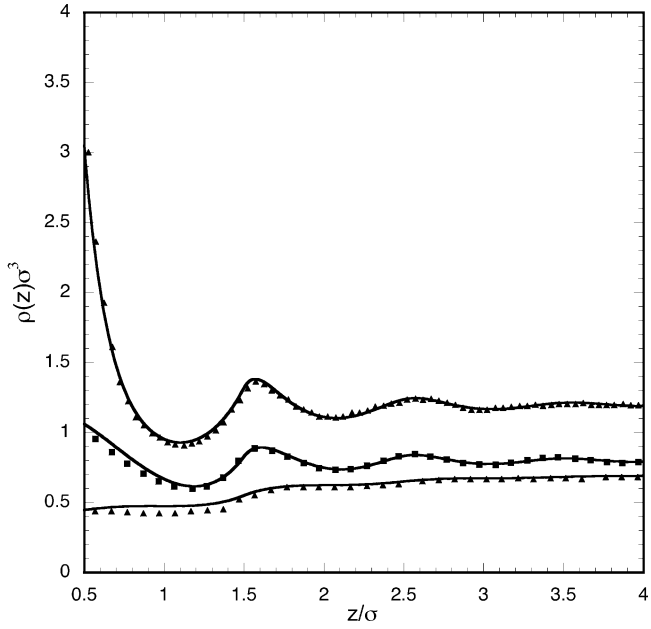

Figure 3. Density profiles for an attractive Yukawa fluid near a single wall. Upper (attractive wall) and lower (hard wall) curves: $\rho^* = 0.70$, $T^* = 1.1$, $\kappa^* = 1.8$ (the results are actually for a wide pore of width $H = 10\sigma$). Medium curve (hard wall): $\rho^* = 0.79984$, $T^* = 0.61$, $\kappa^* = 4$. Solid lines, RFA; triangles, simulation of ref 43; squares, simulation of ref 44.

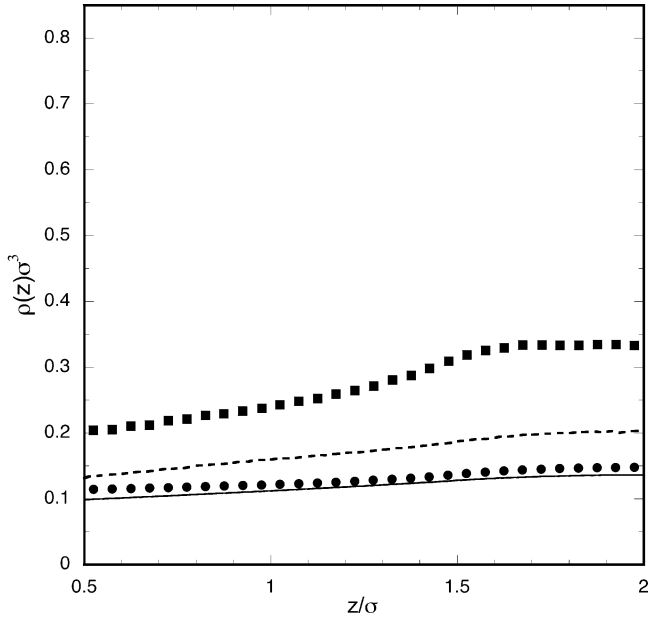

Figure 4. Density profiles for an attractive Yukawa fluid in a slit pore at $\rho^* = 0.70063$ (see text), $T^* = 1.1$, $\kappa^* = 1.8$, and $H = 4\sigma$. Solid line, RFA; dashed line, results of the DFT of ref 41. Simulations: circles[42] and squares.[44]

above from the no-solution problem. This limitation becomes especially severe for the NAHS mixture with high composition asymmetry. Since the Δb closure gives acceptable results over the relevant range of concentrations, as shown above, we used it *faute de mieux* to study the structure of the confined fluid. In Figures 5 and 6, the density profiles computed from the Δb/RFA integral equation (standing for the bulk/pore closures) are compared with MC simulation. Except for the largest concentration and the immediate vicinity of the walls, the computed density profiles are in perfect agreement with simulations for this value of the total density. Since the PINBI effect occurs

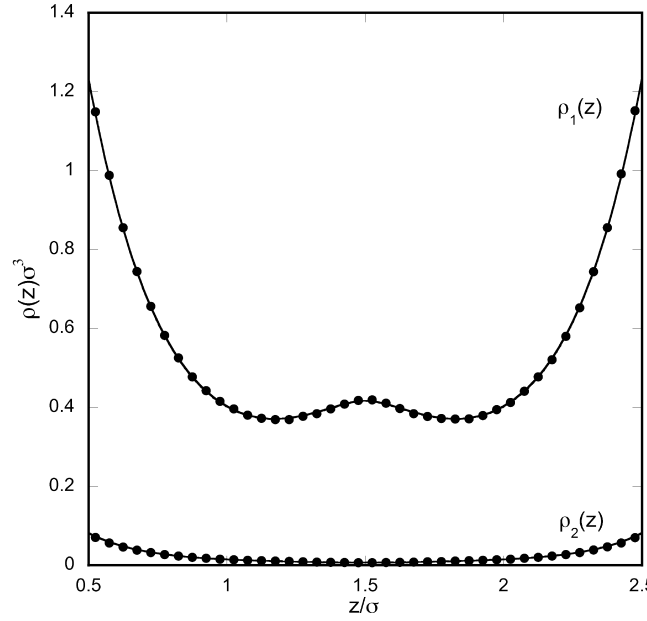

Figure 5. Density profiles of a NAHS mixture in a slit pore. The parameters are $\delta = 0.2$, $\rho^* = 0.45$, $x_2 = 0.02$, and $H = 3\sigma$. Solid lines, Δb/RFA; symbols, MC.[42]

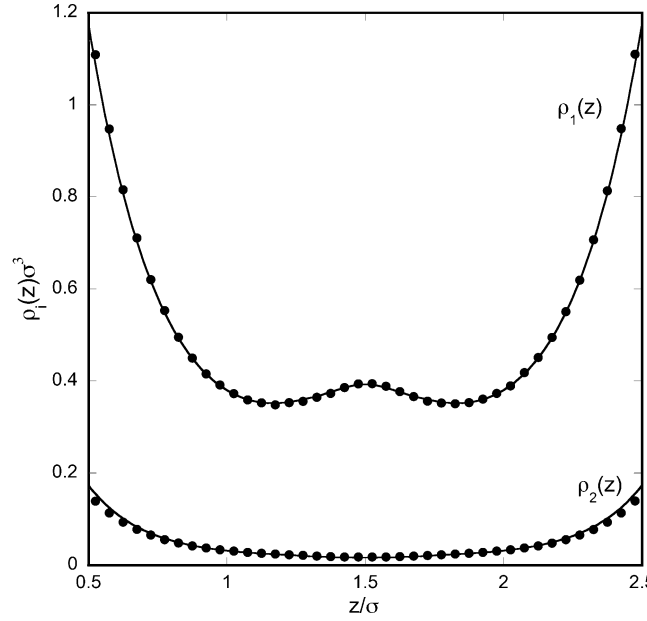

Figure 6. Density profiles of the NAHS mixture in a slit pore. The parameters are $\delta = 0.2$, $\rho^* = 0.45$, $x_2 = 0.04$, and $H = 3\sigma$. Solid lines, Δb/RFA; symbols, MC.[42]

for conditions not so far from these, it seems reasonable to examine the adsorption predicted by the Δb/RFA IE.

3.2.3. Adsorption. Adsorption curves for the NAHS mixture obtained from simulations are available for $H = 3\sigma$.[21] Slightly before the threshold density, the full RFA closure is no longer convergent ($\rho^* \simeq 0.53$ for example without optimization). We thus compare the MC data with the Δb/RFA ones in Figure 7 for the most asymmetric mixture, $x_2 = 0.02$. In this specific case, the threshold density for the jump in adsorption is very accurately determined from the Δb/RFA integral equation. The value of the adsorption before the threshold is also very accurate, somewhat less so beyond, partly because the bulk becomes then demixed (see the discussion in ref 21 of this population inversion in relation with the bulk instability). Figure 7b which details the region near the threshold shows that while the PY/HNC

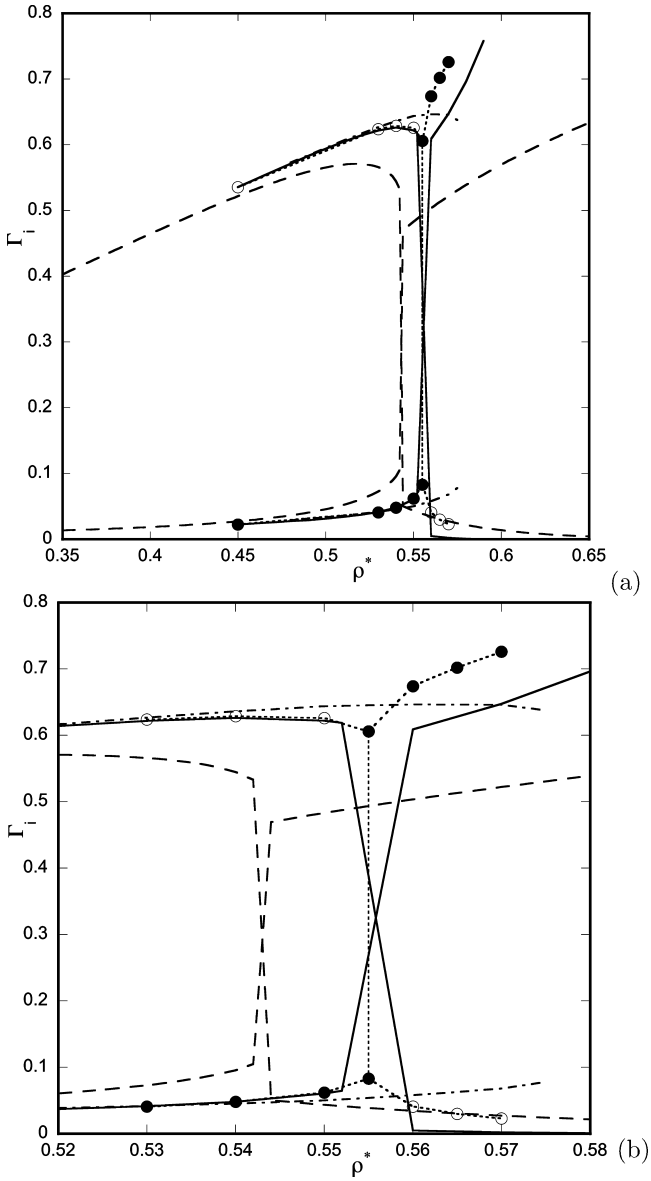

Figure 7. Adsorption curve of an NAHS mixture in a slit pore. The parameters are $\delta = 0.2$, $x_2 = 0.02$, and $H = 3\sigma$. Solid lines, Δb/RFA; dashed lines, PY/HNC; dotted-dashed lines, Martynov−Sarkisov;[45] symbols, MC.[20,21] The dotted lines between the MC data are guides to the eye.

estimate is acceptable, the adsorption/desorption curves are somewhat less so (see also ref 18 for more results with this closure). In Figures 8 and 9, the adsorption is shown at an enlarged scale at two higher concentrations $x_2 = 0.03$ and $x_2 = 0.04$. The Δb/RFA IE still predicts within a few percents the threshold density for the PINBI. The transitions occur however at slightly lower densities, with the adsorption curves being also steeper (the critical density for the PINBI is underestimated). To check the effect of the wall−particle closure, we also show in Figure 7 the adsorption computed with the Δb/MS closure, using *in the pore* the Martynov−Sarkisov closure.[45] In this case, with the same bulk structure, the jump occurs after the simulation one. This shows that a good determination of the threshold requires both good bulk dcfs and an accurate closure in the pore.

4. Conclusion

In this work, we have examined the adsorption of nonadditive hard spheres confined in a slit pore as a function of the bulk

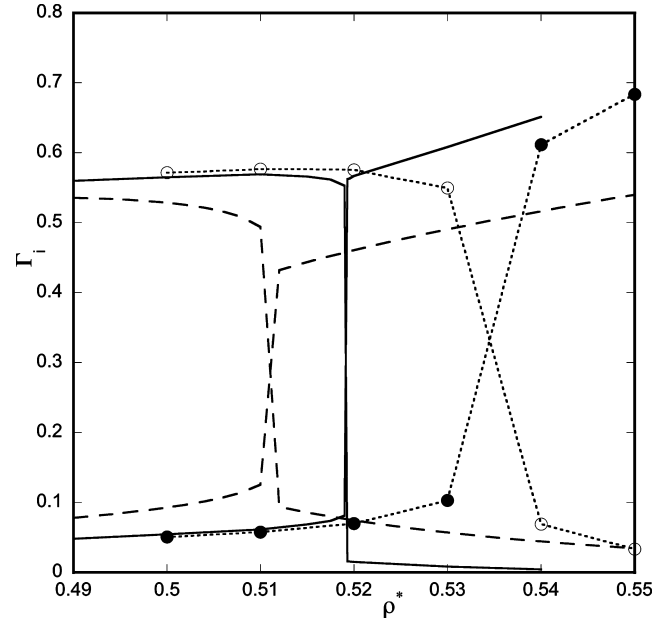

Figure 8. Adsorption curve of an NAHS mixture in a slit pore. The parameters are $\delta = 0.2$, $x_2 = 0.03$, and $H = 3\sigma$. Solid lines, Δb /RFA; dashed lines, PY/HNC; symbols, MC.[42] The dotted lines between the MC data are guides to the eye.

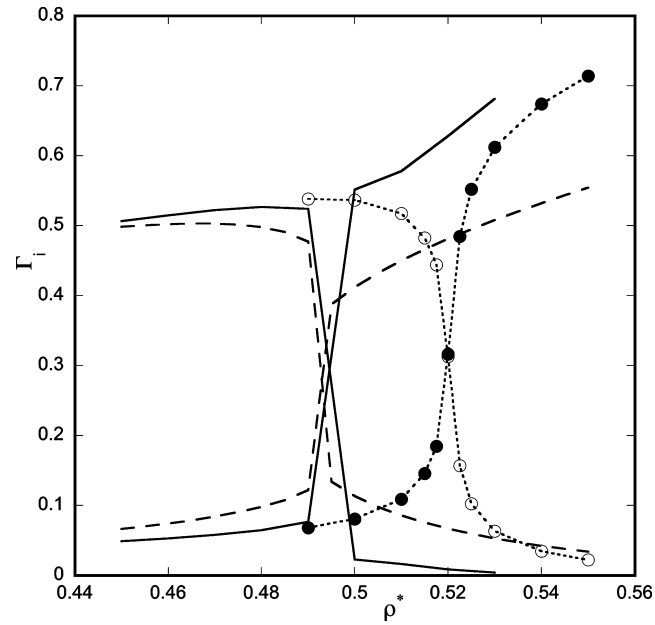

Figure 9. Adsorption curve of an NAHS mixture in a slit pore. The parameters are $\delta = 0.2$, $x_2 = 0.04$, and $H = 3\sigma$. Solid lines, Δb /RFA; dashed lines, PY-HNC; symbols, MC.[20,21] The dotted lines between the MC data are guides to the eye.

composition and total density. We have shown that the approximate closure we have proposed to overcome the nonconvergence problem of the integral equations with full reference functional bridge functions predicts within a few percents the threshold density for the population inversion. Of course, for this specific model, the same result can be obtained directly by performing the simulation, with a comparable numerical cost, since it suffices then to check for the overlap of the cores. This is no longer the case for more complex interaction potentials. As an example, the confined mixture of hard spheres and dipolar hard spheres on which the field induced population inversion has been shown requires several days of simulation just to have a single point on the adsorption isotherms. It is then difficult to

investigate with simulations a wide domain of the parameters space. The difference in numerical cost between the semianalytic methods and the simulation becomes then more significant. We think that it is then useful to continue the effort for developing such methods for more complex models than the nonadditive hard sphere mixture. It should thus be possible, for example, to extend the existing treatments by integral equations of dipolar fluids in order to examine the effect of an external field in confined geometry. The possibility to map in a reasonable time a sufficient domain of the parameters space (bulk composition, size ratios, dipole moments, field strength, pore width, etc.) would help to focus the simulation only in the useful part of this space, for quantitative studies or for providing guidelines to experimental studies.

Acknowledgment. The authors are grateful to Charles Brunet for providing Monte Carlo data complementary to those given in refs 20 and 21 and to Jean-Guillaume Malherbe for those for the Yukawa fluid and useful discussions.

Appendix A

The Reference Functional Approximation

From the functional Taylor expansion of the excess free energy functional $F^{ex}[\rho]$ about some reference density ρ_0, the bridge functional is defined as[22]

$$F^{B}[\rho] \equiv F^{ex}[\rho] - F^{(2)}[\rho] \tag{A-1}$$

where the so-called hypernetted chain (HNC) functional $F^{(2)}[\rho]$ contains the contributions up to second order. In the reference functional approximation, F^{B} is replaced by the bridge functional of a reference system, $F^{B,ref}$, for which $F^{ex,ref}$ (and hence also $F^{(2),ref}$) is known:

$$F^{B,ref}[\rho] \equiv F^{ex,ref}[\rho] - F^{(2),ref}[\rho] \tag{A-2}$$

In the fundamental measures theory[22] for additive hard spheres, the excess functional is taken as

$$F^{ex,HS}[\{\rho_i(\mathbf{r})\}] = k_B T \int d\mathbf{x}\, \Phi(\{n_\alpha(\mathbf{x})\}) \tag{A-3}$$

where $\{n_\alpha(\mathbf{x})\}$ is a set of weighted densities constructed from the actual densities $\rho_i(r)$ and weight functions $\omega_i^{(\alpha)}$ as $n_\alpha(\mathbf{x}) = \sum_i \rho_i \otimes \omega_i^{(\alpha)}$, where $\otimes$ designates the convolution product. From $F^{ex,ref}[\rho]$ (where ref means HS or NAHS), one evaluates the coefficients $c_i^{(1),ref}$ and $c_{ij}^{(2),ref}$ of the functional $F^{(2),ref}$ (one- and two-particle dcfs) and thus determines $F^{B,ref}$. The excess free energy in the RFA is thus

$$F^{ex}[\rho] \simeq F^{(2)}[\rho] + F^{B,ref}[\rho] \tag{A-4}$$

Appendix B

Bridge Function in the Test Particle Limit of the RFA

From the definition of the bridge functional, one computes the bridge functions as $b_{it}(r) = \beta[(\delta F^{B})/(\delta \rho_i(\mathbf{r}))]|_{\rho_i = \rho_0 g_{ij}}$. In the RFA, one uses $F^{B,ref}$ defined in eq A-2 in place of the unknown F^{B}. Explicit expressions for computing the bridge function with the original FMF are given in the Appendix of ref 22. We summarize here the main quantities required in the modified version given in ref 46. The free energy density $\Phi(\{n_\alpha\})$ consistent with the BMCSL equation[47] (superscript CS) contains scalar and vector contributions:

$$\Phi^{CS}[\{n_\alpha(\mathbf{r})\}] = \Phi^{S(CS)}[\{n_\alpha(\mathbf{r})\}] + \Phi^{V(CS)}[\{n_\alpha(\mathbf{r})\}] \tag{B-1}$$

$$\Phi^{S(CS)} = -n_0 \ln(1 - n_3) + \frac{n_1 n_2}{1 - n_3} + \frac{1}{36\pi}\left[\frac{1}{n_3^{\,2}} \ln(1 - n_3) + \frac{1}{n_3 (1 - n_3)^2}\right] n_2^{\,3} \tag{B-2}$$

$$\Phi^{V(CS)} = -\frac{\mathbf{n}_{V_1} \cdot \mathbf{n}_{V_2}}{1 - n_3} - \frac{1}{12\pi}\left[\frac{1}{n_3^{\,2}} \ln(1 - n_3) + \frac{1}{n_3 (1 - n_3)^2}\right] n_2 \mathbf{n}_{V_2} \cdot \mathbf{n}_{V_2} \tag{B-3}$$

The weighted densities are computed in Fourier space as $\tilde{n}_\alpha(\mathbf{k}) = \sum_i \rho_i(\mathbf{k}) \tilde{\omega}_i^{(\alpha)}(-\mathbf{k})$, where the Fourier transforms of the weight functions $\tilde{\omega}_i^{(\alpha)}$ are

$$\frac{\tilde{\omega}_i^{(q)}(k)}{R_i^{(q)}} = \frac{\sin(kR_i)}{kR_i}, \quad q = 0, 1, 2$$

$$\frac{\tilde{\omega}_i^{(3)}(k)}{R_i^{(3)}} = 3\frac{\sin(kR_i) - kR_i \cos(kR_i)}{(kR_i)^3}$$

$$\tilde{\omega}_i^{(V_2)}(\mathbf{k}) = (-1)^{1/2} \mathbf{k} \tilde{\omega}_i^{(3)}(k), \quad \tilde{\omega}_i^{(V_1)}(\mathbf{k}) = \frac{\tilde{\omega}_i^{(V_2)}(\mathbf{k})}{4\pi R_i} \tag{B-4}$$

with $R_i^{(q)} = 1$ and R_i, S_i, V_i for $q = 0$, 1, 2, 3 (R_i, S_i, and V_i denote the hard sphere radius, the surface area, and the volume of the sphere of species i, respectively).

The bridge functions are computed from

$$b_{ij}[\{\rho_i(\mathbf{r});\mathbf{r}\}] = \beta\left(\mu_i^{ex,HS}[\{\rho_i g_{ij}(\mathbf{r});\mathbf{r}\}] - \mu_i^{ex,HS}(\{\rho_i\})\right) + \sum_k \rho_k c_{ik}^{(2),HS} \otimes h_{kj}(r) \tag{B-5}$$

with

$$c_i^{(1)}(r) = -\beta \mu_i^{ex,HS}[\{\rho_i(r)\};\mathbf{r}] = -\int d\mathbf{r}' \sum_\alpha \mu_\alpha[\{n_\alpha(r')\};r] \omega_i^{(\alpha)}(\mathbf{r}' - \mathbf{r})$$

$$\mu_\alpha[\{n_\alpha(\mathbf{r})\}] = \frac{\partial \Phi}{\partial n_\alpha}$$

and

$$-c_{ij}^{(2),\mathrm{HS}}(\mathbf{r}) = \sum_{\alpha,\gamma} \Phi_{\alpha,\gamma} \int \mathrm{d}\mathbf{r}'\, \omega_i^{(\alpha)}(\mathbf{r}')\, \omega_j^{(\gamma)}(\mathbf{r}' - \mathbf{r})$$
$$-\tilde{c}_{ij}^{(2)}(k) = \sum_{\alpha,\gamma} \Phi_{\alpha,\gamma}\, \tilde{\omega}_i^{(\alpha)}(\mathbf{k})\, \tilde{\omega}_j^{(\gamma)}(-\mathbf{k})$$
$$\Phi_{\alpha,\gamma} = \left[\frac{\partial^2 \Phi}{\partial n_\alpha \partial n_\gamma}\right]_{\{n_{\alpha,0}\}} \tag{B-6}$$

References and Notes

(1) *Fundamentals of Adsorption 1993: Proceedings of the Fourth International Conference on Fundamentals of Adsorption, Kyoto*; Suzuki, M., Ed.; Elsevier: Amsterdam, 1993.
(2) Hansen, J. P.; McDonald, I. R. *Theory of Simple Liquids*; Academic: London, 1976.
(3) Gazzillo, D. *J. Chem. Phys.* **1991**, *95*, 4565.
(4) Lomba, E.; Alvarez, M.; Lee, L. L.; Almarza, N. G. *J. Chem. Phys.* **1996**, *104*, 4180.
(5) Jagannathan, K.; Reddy, G.; Yethiraj, A. *J. Phys. Chem. B* **2005**, *109*, 6764.
(6) Amar, J. G. *Mol. Phys.* **1987**, *67*, 739.
(7) Jagannathan, K.; Yethiraj, A. *J. Chem. Phys.* **2003**, *118*, 7907.
(8) Kahl, G.; Bildstein, B.; Rosenfeld, Y. *Phys. Rev. E* **1996**, *54*, 5391.
(9) Lo Verso, F.; Pini, D.; Reatto, L. *J. Phys.: Condens. Matter* **2005**, *17*, 771.
(10) Schmidt, M. *J. Phys.: Condens. Matter* **2004**, *16*, L351.
(11) Paricaud, P. *Phys. Rev. E* **2008**, *78*, 021202.
(12) Ayadim, A.; Amokrane, S. *J. Phys.: Condens. Matter* **2010**, *22*, 035103.
(13) Sillren, P.; Hansen, J. P. *Mol. Phys.* **2010**, *108*, 97.
(14) Santos, A.; Lopez de Haro, M.; Yuste, S. B. *J. Chem. Phys.* **2010**, *132*, 204506.
(15) Duda, Y.; Vakarin, E. V.; Alejandre, J. *J. Colloid Interface Sci.* **2003**, *258*, 10.
(16) Duda, Y.; Pizio, O.; Sokolowski, S. *J. Phys. Chem. B* **2004**, *108*, 19442.
(17) Jiménez-Angeles, F.; Duda, Y.; Odriozola, G.; Lozada-Cassou, M. *J. Phys. Chem. C* **2008**, *112*, 18028.
(18) Kim, S.; Suh, S.; Seong, B. *J. Korean Phys. Soc.* **2009**, *54*, 60.
(19) Gozdz, W. T. *J. Chem. Phys.* **2005**, *122*, 074505.
(20) Brunet, C.; Malherbe, J. G.; Amokrane, S. *J. Chem. Phys.* **2009**, *131*, 221103.
(21) Brunet, C.; Malherbe, J. G.; Amokrane, S. *Phys. Rev. E* **2010**, *82*, 021504.
(22) Rosenfeld, Y. *J. Chem. Phys.* **1993**, *98*, 8126.
(23) Wu, J. *Thermodynamics* **2006**, *52*, 1169.
(24) Roth, R. *J. Phys.: Condens. Matter* **2010**, *22*, 063102.
(25) Zhou, S. *Chem. Rev.* **2009**, *109*, 2829.
(26) Rosenfeld, Y. *Phys. Rev. Lett.* **1994**, *72*, 3831.
(27) Rosenfeld, Y. *Mol. Phys.* **1998**, *94*, 929.
(28) Amokrane, S.; Malherbe, J. G. *J. Phys.: Condens. Matter* **2001**, *13*, 7199. *Erratum* Amokrane, S.; Malherbe, J. G. *J. Phys.: Condens. Matter* **2002**, *14*, 3845.
(29) Ayadim, A.; Malherbe, J. G.; Amokrane, S. *J. Chem. Phys.* **2005**, *122*, 234908.
(30) Amokrane, S.; Ayadim, A.; Malherbe, J. G. *J. Phys. Chem. C* **2007**, *111*, 15982.
(31) Oettel, M. *J. Phys.: Condens. Matter* **2005**, *17*, 429.
(32) Mognetti, B.; Oettel, M.; Yelash, L.; Virnau, P.; Paul, W.; Binder, K. *Phys. Rev. E* **2008**, *77*, 041506.
(33) Ayadim, A.; Oettel, M.; Amokrane, S. *J. Phys.: Condens. Matter* **2009**, *21*, 115103.
(34) Lado, F. *Phys. Rev. A* **1973**, *8*, 2548.
(35) Lado, F.; Foiles, S. M.; Ashcroft, N. W. *Phys. Rev. A* **1983**, *28*, 2374. Lado, F. *Phys. Lett.* **1982**, *89*, 196.
(36) Brey, J. J.; Santos, A. *Mol. Phys.* **1986**, *57*, 149.
(37) Belloni, L. *J. Chem. Phys.* **1993**, *98*, 8080.
(38) Anta, J. A. *J. Phys.: Condens. Matter* **2005**, *17*, 7935. Anta, J. A.; Bresme, F.; Lago, S. *J. Phys.: Condens. Matter* **2003**, *15*, S3491.
(39) Amokrane, S.; Ayadim, A.; Malherbe, J. G. *J. Chem. Phys.* **2005**, *123*, 174508.
(40) Amokrane, S.; Ayadim, A.; Malherbe, J. G. *Mol. Phys.* **2006**, *104*, 3419.
(41) Zhou, S. *J. Chem. Phys.* **2009**, *131*, 134702.
(42) Brunet, C.; Malherbe, J. G. Unpublished work.
(43) You, F.; Fu, S.; Yu, Y.; Gao, G. *J. Phys. Chem. B* **2005**, *109*, 3512.
(44) Zhou, S.; Jamnik, A. *J. Chem. Phys.* **2005**, *122*, 064503.
(45) Martynov, G. A.; Sarkisov, G. N. *Mol. Phys.* **1983**, *49*, 1495.
(46) Roth, R.; Evans, R.; Lang, A.; Kahl, G. *J. Phys.: Condens. Matter* **2002**, *14*, 12063.
(47) Boublik, T. *J. Chem. Phys.* **1970**, *53*, 471. Mansoori, G. A.; Carnahan, N. F.; Starling, K. E.; Leland, T. W., Jr. *J. Chem. Phys.* **1971**, *54*, 1523.

JP107157A